Supplementary Information

Transient control of lytic activity via non-equilibrium chemical reaction system

Kohei Sato,*[‡a§] Yume Nakagawa,[‡a] Miki Mori,[a] Masahiro Takinoue,[bca] and Kazushi Kinbara*[ac]

[a]*School of Life Science and Technology,* [b]*Department of Computer Science,* [c]*Living Systems Materialogy Research Group, International Research Frontiers Initiative, Tokyo Institute of Technology, 4259 Nagatsuta-cho, Midori-ku, Yokohama 226-8501, Japan;* [§]*Present address: Department of Chemistry, School of Science, Kwansei Gakuin University, 1 Gakuen Uegahara, Sanda-shi, Hyogo 669-1330, Japan*

*To whom correspondence should be addressed. ksato@kwansei.ac.jp (K.S.);
kkinbara@bio.titech.ac.jp (K.K.)
‡These authors contributed equally to this work.

Table of Contents

1. General

Unless otherwise noted, all commercial reagents were used as received. ^{1}H and ^{13}C NMR spectra were recorded on a Varian model 400-MR spectrometer and a JEOL model JNM-ECZL400S spectrometer operating at 400 MHz for ^{1}H and 100 MHz for ^{13}C NMR, respectively. The chemical shifts were determined with respect to tetramethylsilane (TMS) or a residual non-deuterated solvent as an internal reference. Electrospray ionization time-of-flight (ESI-TOF) mass spectrometry was performed on a Bruker model microTOF II spectrometer. Electron ionization (EI) mass spectrometry was performed on a JEOL model JMS-700 MStation spectrometer. Reverse-phase high-performance liquid chromatography (RP-HPLC) was performed on a Shimadzu model Prominence system using a 20 I.D. x 250 mm Cosmosil $5C_{18}$-AR-II packed column at room temperature. Ultra-performance liquid chromatography (UPLC) was performed on a Waters model ACQUITY Premier system equipped with a tunable UV (TDV) detector using a 2.1 I.D. x 50 mm ACQUITY Premier BEH C_{18} column attached to VanGuard™FIT. Dynamic light scattering (DLS) was performed on a Malvern model Zetasizer Nano ZSP spectrophotometer using a disposable plastic microcuvette with an optical path length of 10 mm. Transmission electron microscopy (TEM) was performed on a JEOL model JEM-1400 electron microscope equipped with C4742-95-12ER camera operating at 100 kV. Surface tension measurements were performed on a KRSUU model DAS100 tensiometer. Fluorescence microscopic observations were performed on an Oympus model IV-71 microscope equipped with U-MWU2 mirror unit (excitation filter: λ = 330–385 nm, emission filter: λ = 420 nm, dichroic mirror: λ = 400 nm). A 0.1 mm thick silicon-based spacer was placed between a slide glass and a coverslip for imaging. Fluorescence spectra were recorded on a JASCO model FP-8550 spectrofluorometer using a quartz cell with an optical path length of 10 mm. Optical density was recorded on a PerkinElmer model multi-label plate reader EnSpire 2300-00J using 96 well black/clear bottom microplates. Electronic absorption spectra were recorded on a JASCO model V-650 UV-Vis spectrophotometer using a quartz cell with an optical path length of 5 mm and 1 mm. Kinetic simulation was carried out using MATLAB® R2022b developed by MathWorks. Optical microscopy observation of emulsions were performed on an Agilent Technologies model BioTek Cytation 5 using cell culture microplate (384 well, PS, F-bottom, µClear®, black, CELLSTAR®, Cell-Repellent surface, lid, sterile).

2. Synthesis

2.1. Synthesis of 4-vinylphenol

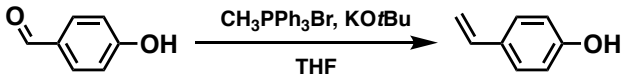

4-vinylphenol was synthesized according to the method analogous to that reported previously.[S1] To a dry THF solution (10 mL) of methyltriphenylphosphonium bromide (5.31 g, 14.9 mmol) and 12 % potassium *tert*-butoxide in THF (ca. 1 M, 21 mL, 21 mmol) was added a dry THF solution (10 mL) of 4-hydroxybenzaldehyde (1.25 g, 10.3 mmol) under Ar at room temperature. After stirring overnight, saturated aqueous NH_4Cl was added to the reaction mixture to quench the reaction and then THF was removed using rotary evaporator. The resulting mixture was extracted five times with CH_2Cl_2 and the organic extract was dried over Na_2SO_4, filtered, and evaporated to dryness under reduced pressure. The obtained residue was subjected to column chromatography on silica gel using *n*-hexane and ethyl acetate (80/20, v/v) as eluent to allow isolation of **4-vinylphenol** as a white solid (1.04 g, 8.63 mmol, 84%). ^{1}H NMR (400 MHz, $CDCl_3$, 25 °C, ppm): δ 7.26 (d, J = 8.4 Hz, 2H), 7.13 (s, 1H), 6.81 (d, J = 8.6 Hz, 2H), 6.62 (dd, J = 17.6, 11.0 Hz, 1H), 5.57 (d, J = 17.6 Hz, 1H), 5.09 (d, J = 10.0 Hz, 1H); ^{13}C NMR (100 MHz, $CDCl_3$, 25 °C, ppm): δ 155.7, 136.3, 130.3, 127.6, 115.5, 111.4.

2.2. Synthesis of ^{Fuel}PEG

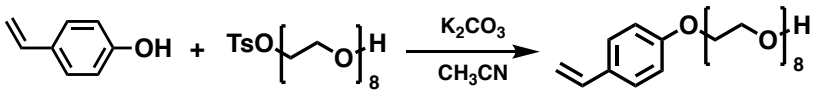

To a dry acetonitrile solution (12.5 mL) of **4-vinylphenol** (478 mg, 3.98 mmol) and octa(ethylene glycol) *p*-toluenesulphonate[S2] (866 mg, 1.65 mmol) was added K_2CO_3 (425 mg, 3.08 mmol) under Ar at room temperature, and the reaction mixture was stirred at 50 °C overnight. Then, the reaction mixture was cooled to room temperature, and celite was added and stirred at room temperature for additional 5 min. The reaction mixture was then filtered and washed with ethyl acetate, and the filtrate was evaporated to dryness under reduced pressure. The obtained residue was subjected to column chromatography on silica gel using ethyl acetate and methanol (100/0 to 80/20, v/v) as eluent to allow isolation of **^{Fuel}PEG** as a pale yellow oil (538 mg, 1.14 mmol, 69%). ^{1}H NMR (400 MHz, $CDCl_3$, 25 °C, ppm): δ 7.33 (d, J = 8.4 Hz, 2H), 6.87 (d, J = 8.8 Hz, 2H), 6.65 (dd, J = 17.5, 10.9 Hz, 1H), 5.60 (dd, J = 17.6, 1.0 Hz, 1H), 5.12 (dd, J = 11.0, 1.0 Hz, 1H), 4.13 (t, J = 4.8 Hz, 2H), 3.85 (t, J = 4.8 Hz, 2H), 3.73-3.60 (m, 28H), 3.08 (br, 1H); ^{13}C NMR (100 MHz, $CDCl_3$, 25 °C, ppm): δ 158.5, 136.1, 130.4, 127.3, 114.5, 111.6, 72.5, 70.7, 70.5, 70.5, 70.2, 69.6, 67.3, 61.6; HRMS (ESI-TOF-MS) *m/z* calcd. for $C_{24}H_{40}O_9Na$ $[M + Na]^+$: *m/z* = 495.2565, found: 495.2560.

2.3. Synthesis of 7-tetradecene

To a dry dichloromethane solution (14 mL) of 1-octene (3.18 g, 28.3 mmol), after being degassed by three freeze-pump-thaw cycles, was added Hoveyda-Grubbs catalyst 2nd generation (HG-II) (81.5 mg, 130 μmol) under Ar at room temperature, and the reaction mixture was stirred overnight at the same temperature. Then, the reaction mixture was evaporated to dryness under reduced pressure. The obtained residue was subjected to column chromatography on silica gel using *n*-hexane as eluent to allow isolation of **7-tetradecene** as a colorless oil (1.47 g, 7.49 mmol, 26%). ^{1}H NMR (400 MHz, $CDCl_3$, 25 °C, ppm): δ 5.38 (s, 2H), 1.96 (s, 4H), 1.27 (s, 16H), 0.86 (s, 6H); ^{13}C NMR (100 MHz, $CDCl_3$, 25 °C, ppm): δ 130.5 (*E* isomer), 130.1 (*Z* isomer), 32.8, 32.7, 31.9, 31.6, 30.0, 29.8, 29.5, 29.1, 29.0, 27.4, 22.8, 22.7, 14.3; LRMS (EI-MS) *m/z* calcd. for $C_{14}H_{28}$ $[M]^+$: *m/z* = 196, found: 196.

2.4. Synthesis of ^{Hyd}PEG

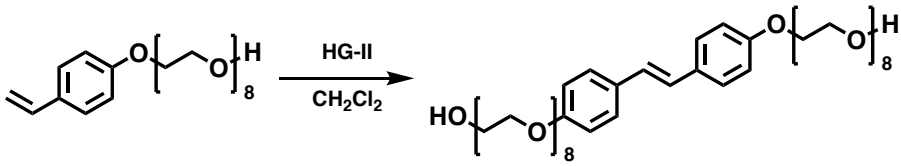

To a dry dichloromethane solution (4.3 mL) of ^{Fuel}**PEG** (545 mg, 1.15 mmol), after being degassed by three freeze-pump-thaw cycles, was added HG-II (67.4 mg, 108 μmol) under Ar at 30 °C, and the reaction mixture was stirred at 40 °C overnight. Then, the reaction mixture was evaporated to dryness under reduced pressure. The obtained residue was subjected to column chromatography on silica gel using chloroform and methanol (95/5, v/v) as eluent. The obtained crude product was further purified by RP-HPLC using methanol and deionized water (0/100 to 100/0, v/v) as eluent to allow isolation of ^{Hyd}**PEG** as a white solid (286 mg, 312 μmol, 54%). ^{1}H NMR (400 MHz, $CDCl_3$, 25 °C, ppm): δ 7.40 (d, J = 8.8 Hz, 4H), 6.92 (s, 2H), 6.89 (d, J = 8.8 Hz, 4H), 4.14 (t, J = 5.2 Hz, 4H), 3.86 (t, J = 4.8 Hz, 4H), 3.74–3.59 (m, 56H), 2.84 (br, 2H); ^{13}C NMR (100 MHz, $CDCl_3$, 25 °C, ppm): δ 158.2, 130.6, 127.4, 126.2, 114.8, 72.6, 70.8, 70.6, 70.6, 70.6, 70.3, 69.7, 67.5, 61.7; HRMS (ESI-TOF-MS) *m/z* calcd. for $C_{46}H_{76}O_{18}Na$ $[M + Na]^+$: *m/z* = 939.4924, found: 939.4928.

2.5. Synthesis of ^{Apm}PEG

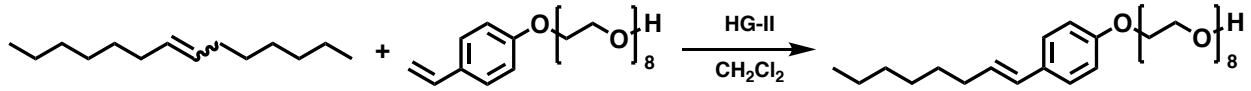

To a dry dichloromethane solution (2.2 mL) of ^{Fuel}**PEG** (103 mg, 218 μmol) and **7-tetradecene** (216 mg, 1.10 mmol), after being degassed by three freeze-pump-thaw cycles, was added HG-II (1.30 mg, 2.07 μmol) under Ar at room temperature, and the reaction mixture was stirred at the same temperature for 1 h. Then, the reaction mixture was evaporated to dryness under reduced pressure. The obtained residue was subjected to column chromatography on silica gel using ethyl acetate and methanol (90/10, v/v) as eluent. The obtained crude product was further purified by RP-HPLC using methanol and deionized water (0/100 to 100/0, v/v) as eluent to allow isolation of ^{Amp}**PEG** as a colorless oil (44.0 mg, 79.0 μmol, 36%). ^{1}H NMR (400 MHz, $CDCl_3$, 25 °C, ppm): δ 7.25 (d, J = 8.8 Hz, 2H), 6.84 (d, J = 8.6 Hz, 2H), 6.30 (d, J = 15.8 Hz, 1H), 6.08 (dt, J = 16.0, 7.2 Hz, 1H), 4.11 (t, J = 4.4 Hz, 2H), 3.84 (t, J = 4.0 Hz, 2H), 3.73–3.58 (m, 28H), 2.17 (q, J = 7.1 Hz, 2H), 1.46-1.30 (m, 8H), 0.89 (t, J = 6.8 Hz, 3H); ^{13}C NMR (100 MHz, $CDCl_3$, 25 °C, ppm): δ 157.8, 131.0, 129.1, 129.0, 126.9, 114.6, 72.8, 70.8, 70.6, 70.5, 70.5, 70.5, 70.5, 70.4, 70.1, 69.7, 67.4, 61.6, 33.1, 31.8, 29.5, 28.9, 22.7, 14.2; HRMS (ESI–TOF–MS) *m/z* calcd. for $C_{30}H_{52}O_9Na$ $[M + Na]^+$: *m/z* = 579.3504, found: 579.3500.

3. Analytical data

3.1. ^{1}H and ^{13}C NMR spectroscopy

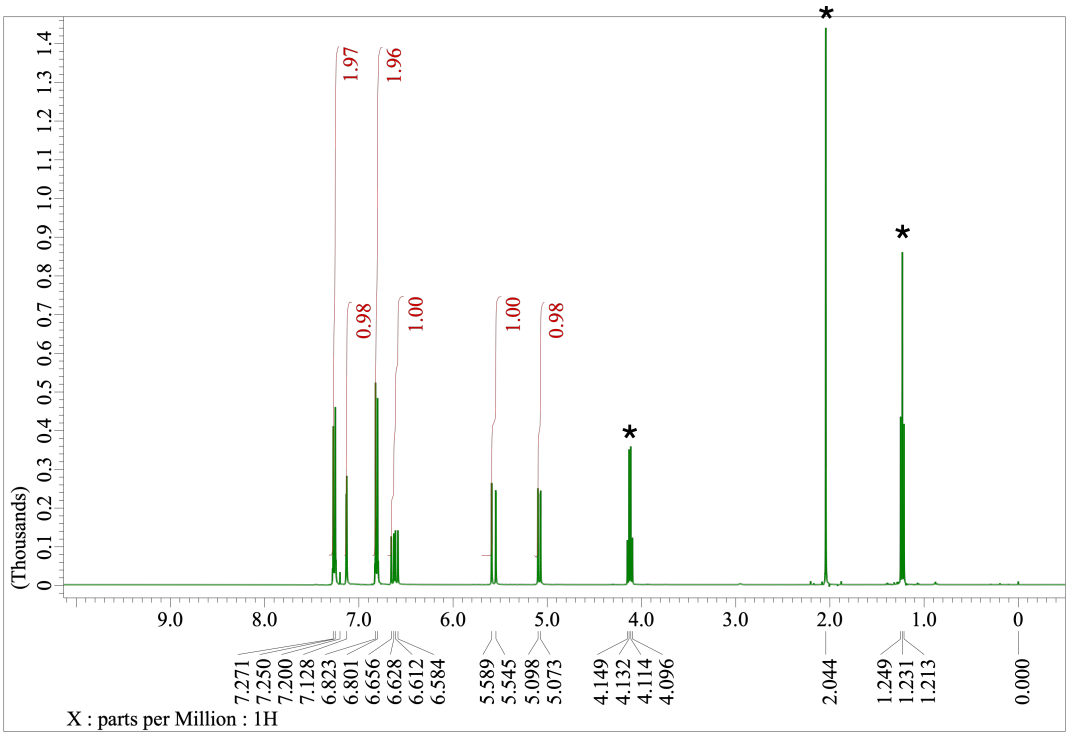

Fig. S1 ^{1}H NMR spectrum (400 MHz) of **4-vinylphenol** in $CDCl_3$ at 25 °C. Asterisks represent solvent peaks.

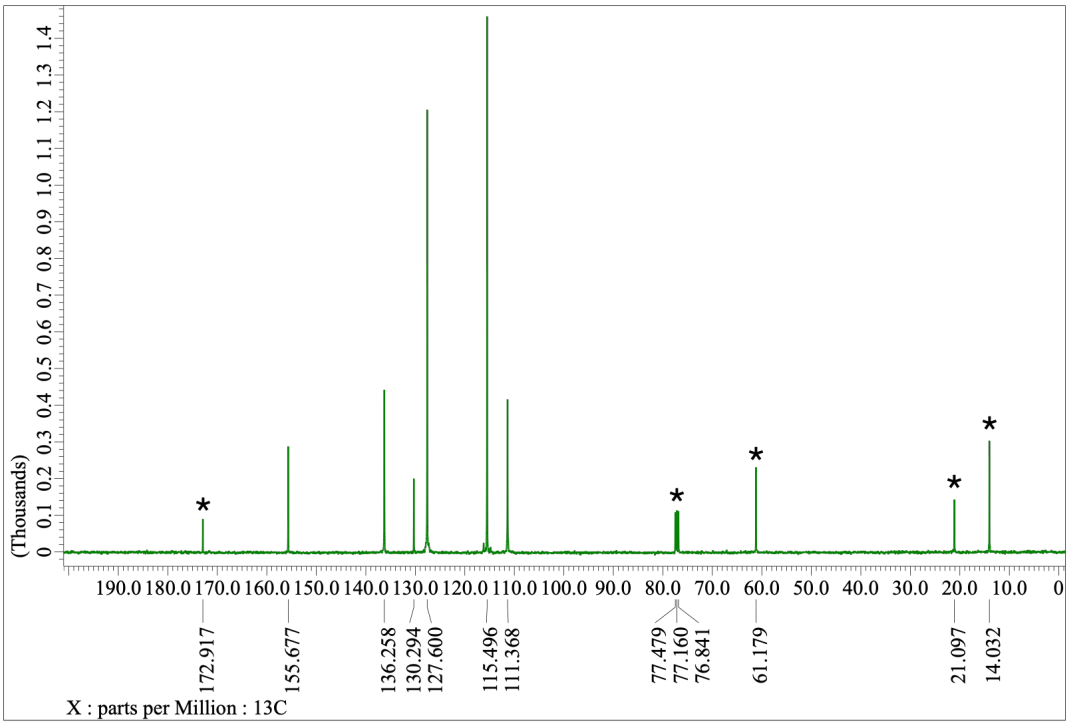

Fig. S2 ^{13}C NMR spectrum (100 MHz) of **4-vinylphenol** in $CDCl_3$ at 25 °C. Asterisks represent solvent peaks.

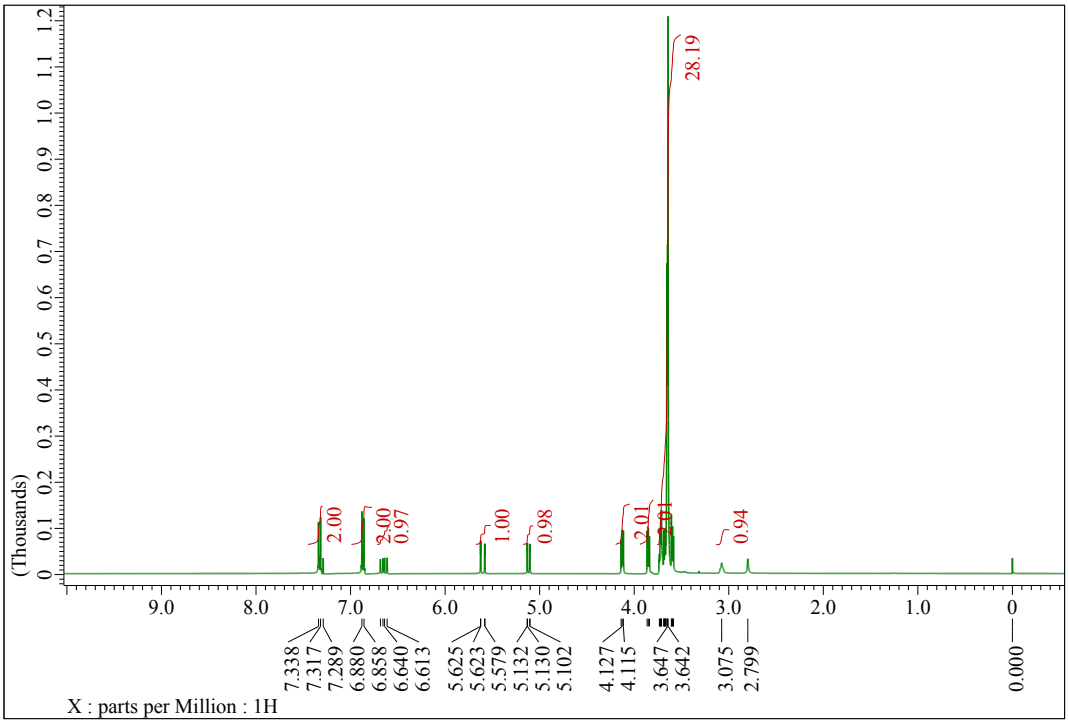

Fig. S3 ^{1}H NMR spectrum (400 MHz) of $^{\mathbf{Fuel}}$**PEG** in $CDCl_3$ at 25 °C.

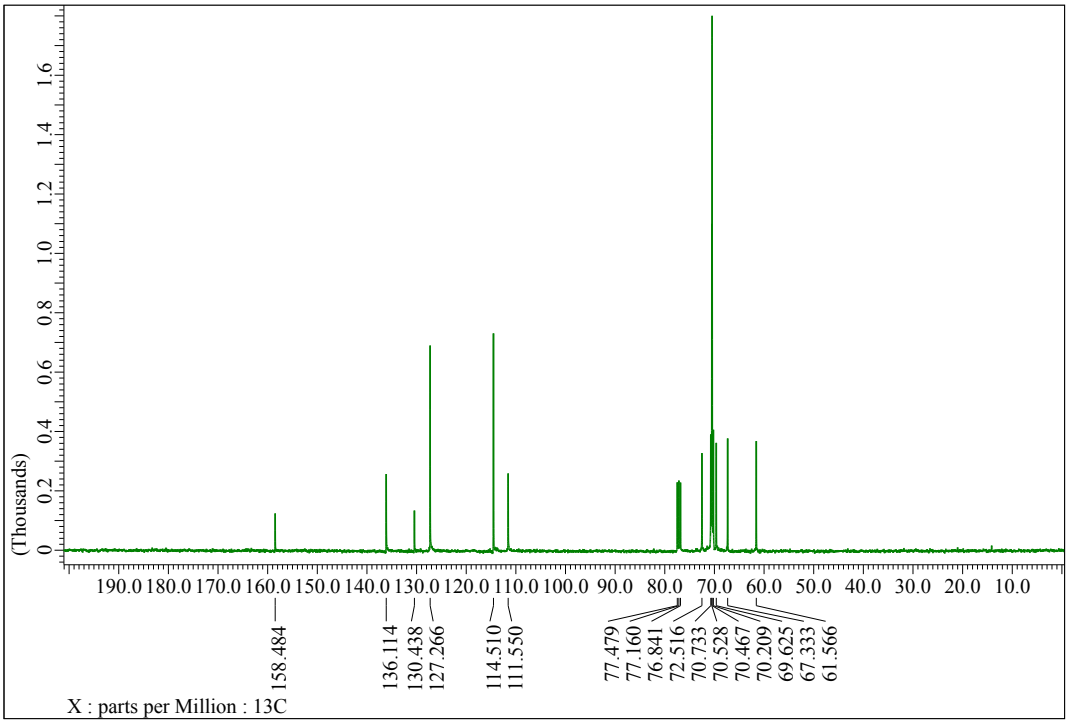

Fig. S4 ^{13}C NMR spectrum (100 MHz) of $^{\mathbf{Fuel}}$**PEG** in $CDCl_3$ at 25 °C.

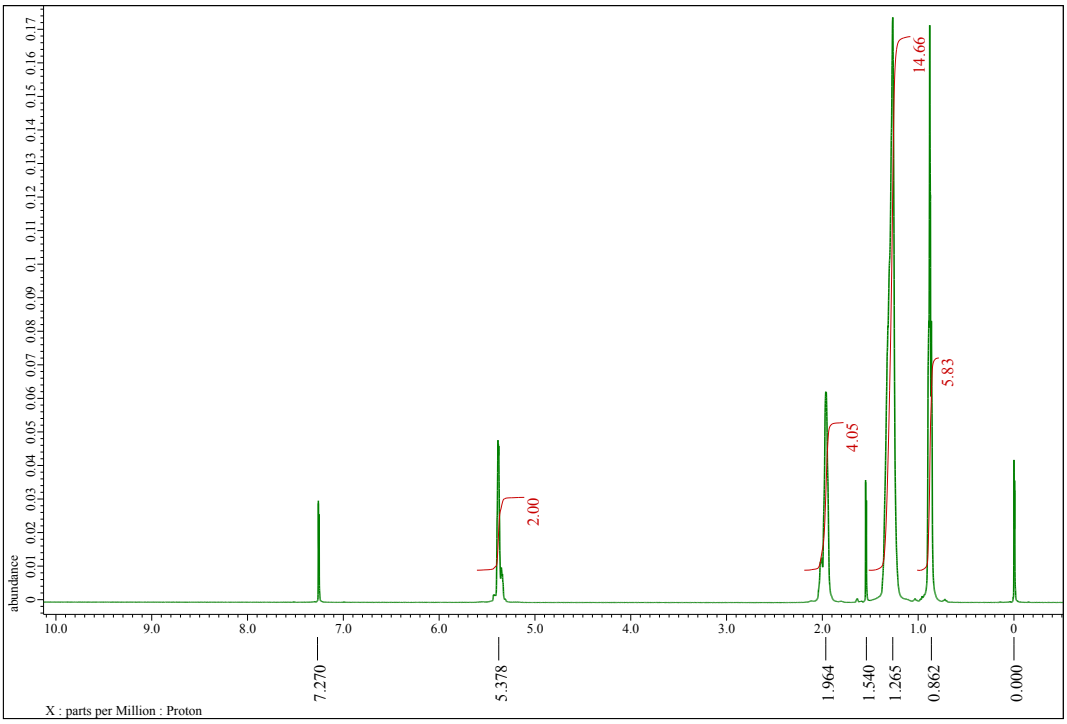

Fig. S5 ^{1}H NMR spectrum (400 MHz) of **7-tetradecene** in $CDCl_3$ at 25 °C.

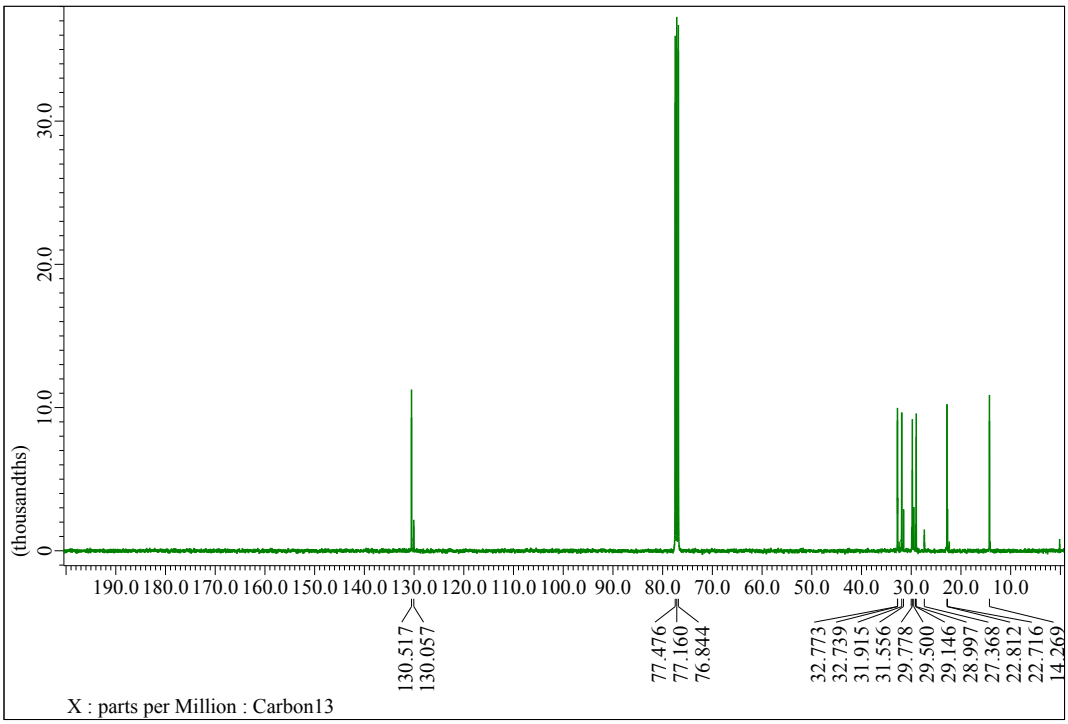

Fig. S6 ^{13}C NMR spectrum (100 MHz) of **7-tetradecene** in $CDCl_3$ at 25 °C.

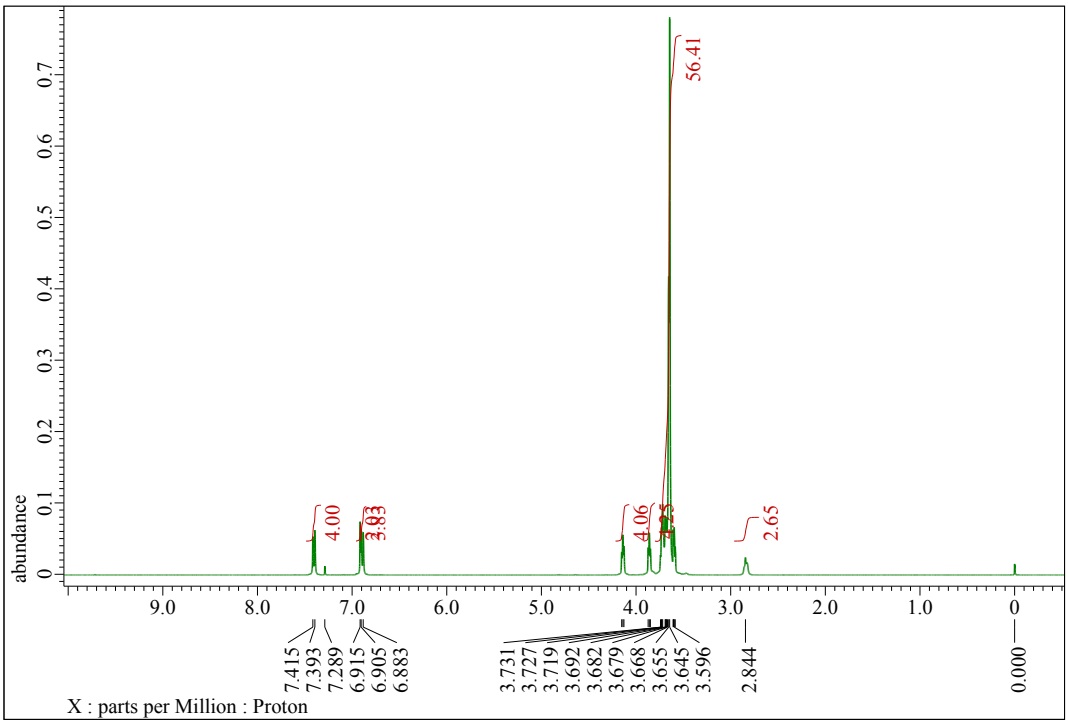

Fig. S7 ^{1}H NMR spectrum (400 MHz) of ^{Hyd}**PEG** in $CDCl_3$ at 25 °C.

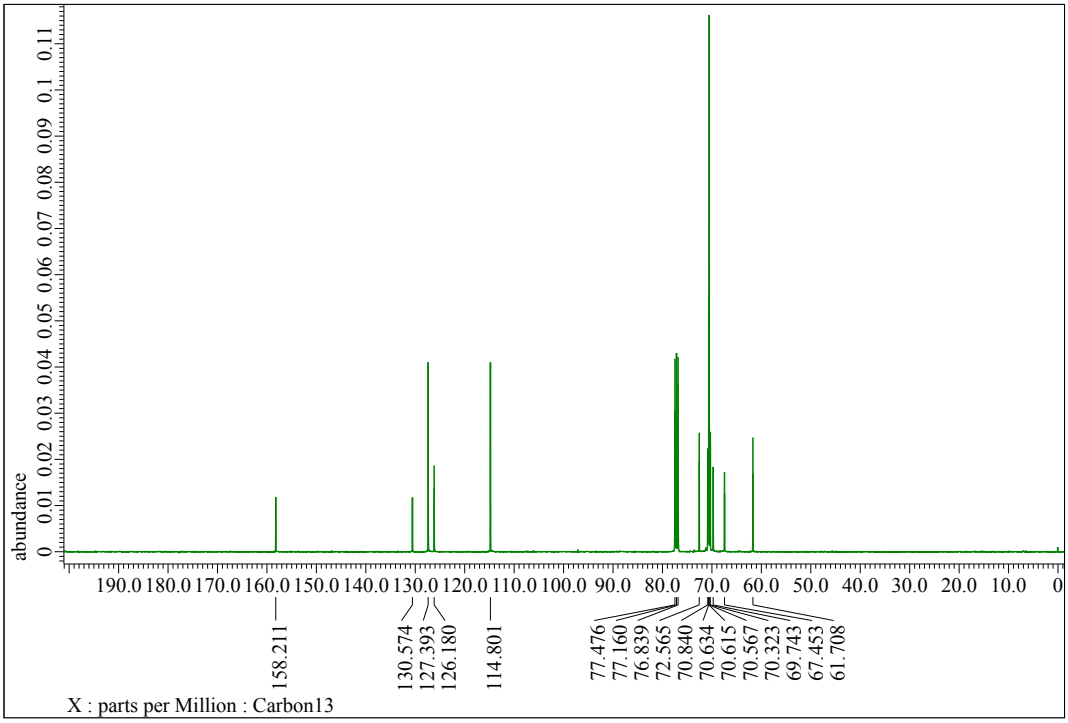

Fig. S8 ^{13}C NMR spectrum (100 MHz) of ^{Hyd}**PEG** in $CDCl_3$ at 25 °C.

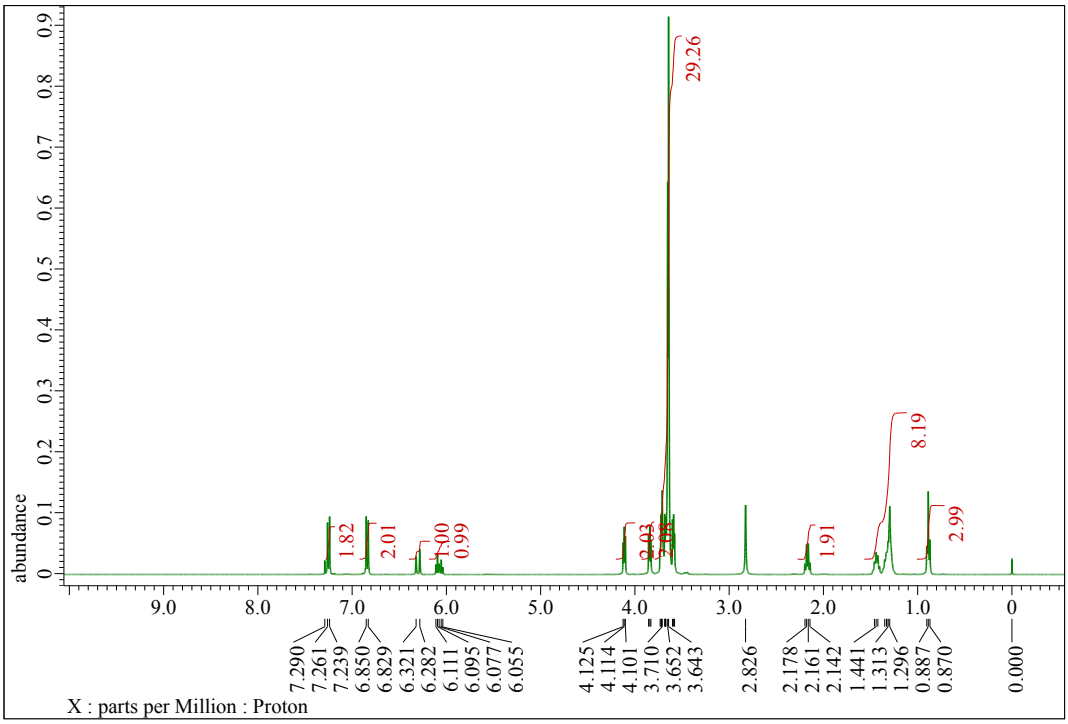

Fig. S9 ^{1}H NMR spectrum (400 MHz) of $^{\mathbf{Amp}}$**PEG** in $CDCl_3$ at 25 °C.

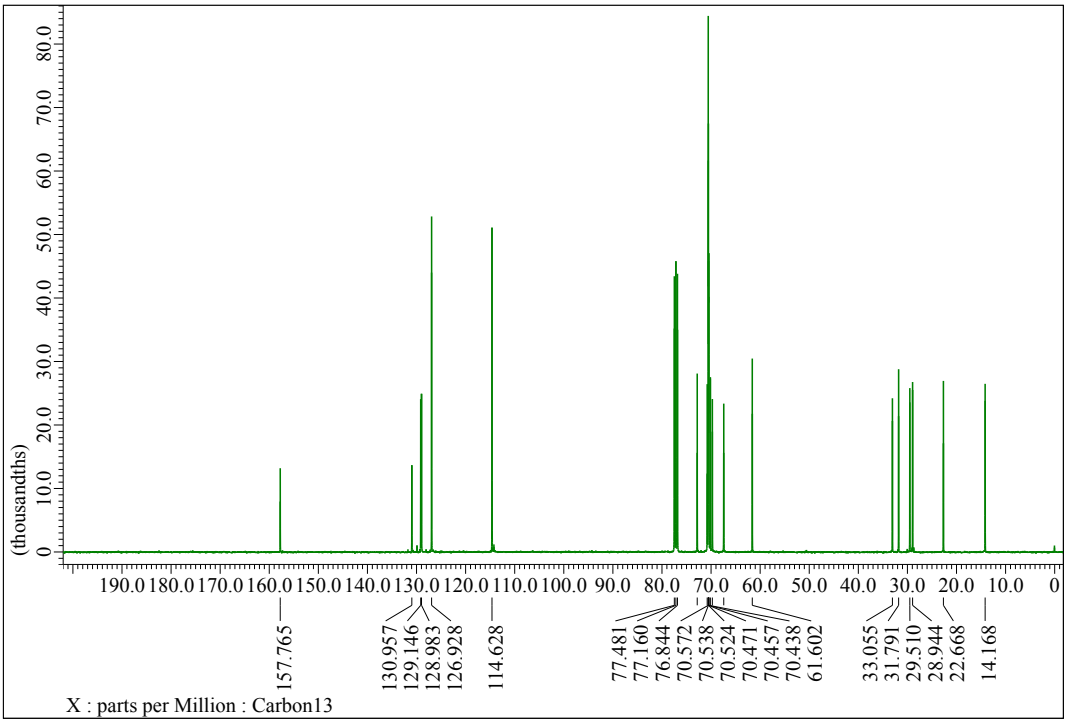

Fig. S10 ^{13}C NMR spectrum (100 MHz) of $^{\mathbf{Amp}}$**PEG** in $CDCl_3$ at 25 °C.

3.2. High-resolution ESI-TOF mass spectrometry

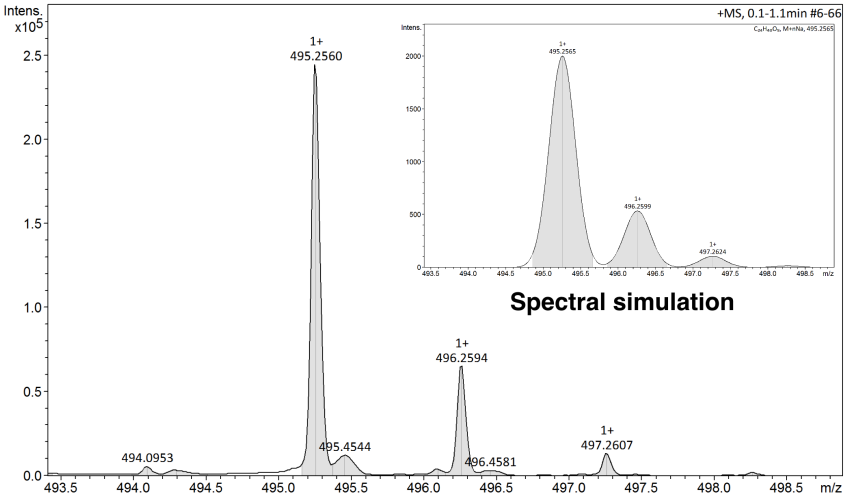

Fig. S11 High-resolution ESI-TOF mass spectrometry of $^{\mathbf{Fuel}}$**PEG**.

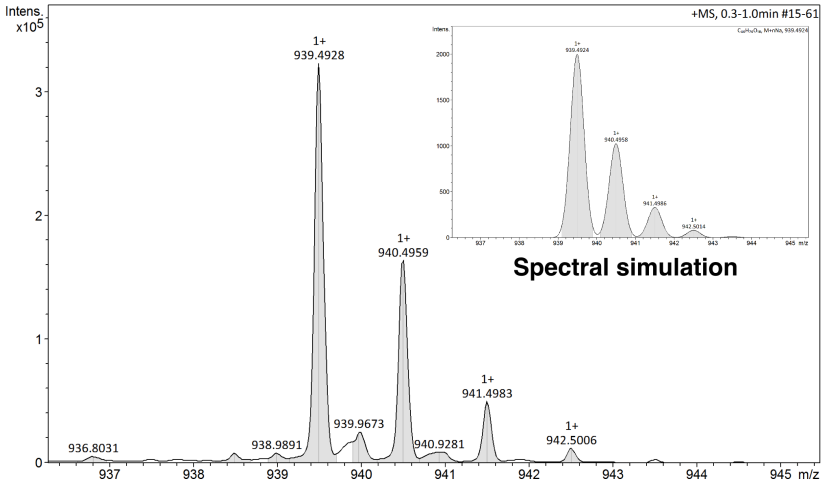

Fig. S12 High-resolution ESI-TOF mass spectrometry of $^{\mathbf{Hyd}}$**PEG**.

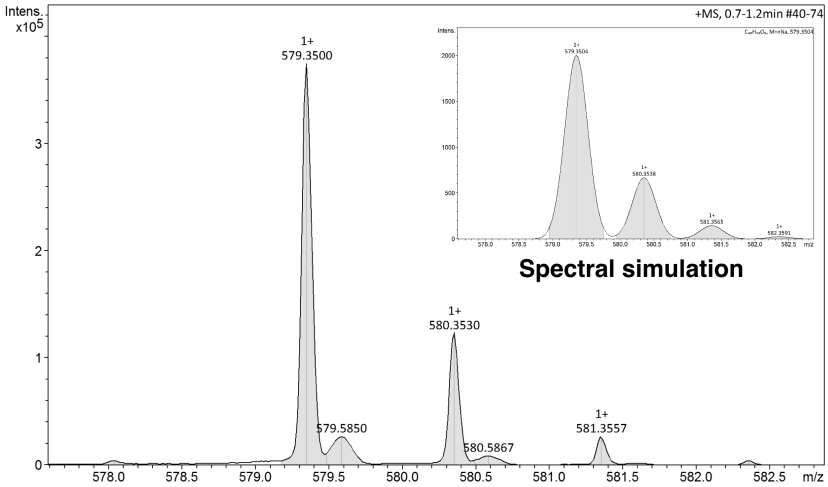

Fig. S13 High-resolution ESI-TOF mass spectrometry of $^{\mathbf{Amp}}$**PEG**.

4. Methods

4.1. Olefin metathesis of ^{Fuel}PEG and 7-tetradecene in CH_2Cl_2

To a dry dichloromethane solution (550 μL) of ^{Fuel}**PEG** (30.1 mg, 63.7 μmol) and **7-tetradecene** (203 mg, 1.04 mmol), after being degassed by three freeze-pump-thaw cycles, was added HG-II (6.50 mg, 10.4 μmol) under Ar at room temperature, and the reaction mixture was stirred at the same temperature and 480 rpm. At each reaction time point, 10 μL of the reaction mixture was diluted with deionized water (500 μL) and analyzed by UPLC (see 4.3.).

4.2. Olefin metathesis of ^{Fuel}PEG and 7-tetradecene in deionized water

To a deionized aqueous solution (550 μL) of ^{Fuel}**PEG** (24.5 mg, 51.8 μmol) and **7-tetradecene** (202 mg, 1.03 mmol), after being degassed by three freeze-pump-thaw cycles, was added HG-II (6.70 mg, 10.7 μmol) under Ar at room temperature, and the reaction mixture was stirred at 50 °C and 480 rpm. At 100 min, a deionized aqueous solution (350 μL) of ^{Fuel}**PEG** (25.4 mg, 53.7 μmol), after being degassed by three freeze-pump-thaw cycles, was added as an additional "fuel". At each time point, the reaction mixture was allowed to stand for 30 s, the bottom aqueous layer was taken using a microsyringe, and 10 μL of the reaction mixture was diluted with deionized water (500 μL) and analyzed by UPLC (see 4.3.).

4.3. Reaction kinetic analyses using UPLC

The diluted reaction mixture (see 4.1. and 4.2.) was vortexed for 10 s, followed by sonication for 3 min. Then, 1.0 μL of the reaction mixture was analyzed by UPLC using methanol and deionized water (5/95 to 95/5, v/v over 5 min, 0.6 mL min^{-1}) as eluent with the detection wavelength of 235 nm. The concentration of each analyte weas calculated from the peak areas.

To calibrate UPLC data, we prepared the standard aqueous solutions of ^{Fuel}**PEG** (10, 20, 50, 80, 100, 120, and 150 mM), ^{Amp}**PEG** (10, 20, 50, 80, and 100 mM), and ^{Hyd}**PEG** (10, 20, 50, 80, and 100 mM) and analyzed them using the same analytical conditions as above. The peak areas were then plotted as a function of the concentration of the analytes to obtain calibration plots (Fig. S14c).

4.4. Qualitative kinetic simulation

First, we listed all the chemical reactions that could occur in our system and formulated the chemical reaction kinetic equations (Table S1). To numerically investigate the chemical reactions, we developed a mathematical model based on a set of simultaneous differential equations shown below where, we set the rate constant k_n to be the same for all reactions and normalized their concentrations based on the initial concentration of 7-tetradecene. The difference between homogeneous and biphasic reactions was conditioned by changing the volume of the aqueous phase. We also assumed

that the ruthenium catalyst was partitioned within the organic phase. Concentration vs. time plots are shown in Fig. S15.

$$\frac{d[F]_{\mathrm{org}}}{dt} = \frac{1}{1+K_F r_V}\left(-2k_1[F]_{\mathrm{org}}^2 - k_2[F]_{\mathrm{org}}[S]_{\mathrm{org}} - k_3[F]_{\mathrm{org}}[A]_{\mathrm{org}} - k_5[F]_{\mathrm{org}}[W]_{\mathrm{org}} + k_{13}[A]_{\mathrm{org}}[W]_{\mathrm{org}} + k_{17}[W]_{\mathrm{org}}[H]_{\mathrm{org}}\right),$$

$$\frac{d[S]_{\mathrm{org}}}{dt} = \frac{1}{1+K_S r_V}\left(-k_2[F]_{\mathrm{org}}[S]_{\mathrm{org}} - k_{10}[S]_{\mathrm{org}}[H]_{\mathrm{org}} + k_{11}[A]_{\mathrm{org}}^2 + k_{13}[A]_{\mathrm{org}}[W]_{\mathrm{org}} + k_{16}[W]_{\mathrm{org}}^2\right),$$

$$\frac{d[A]_{\mathrm{org}}}{dt} = \frac{1}{1+K_A r_V}\left(k_2[S]_{\mathrm{org}}[F]_{\mathrm{org}} - k_3[F]_{\mathrm{org}}[A]_{\mathrm{org}} + k_5[F]_{\mathrm{org}}[W]_{\mathrm{org}} + 2k_{10}[S]_{\mathrm{org}}[H]_{\mathrm{org}} - 2k_{11}[A]_{\mathrm{org}}^2 - k_{13}[A]_{\mathrm{org}}[W]_{\mathrm{org}} + k_{17}[W]_{\mathrm{org}}[H]_{\mathrm{org}}\right),$$

$$\frac{d[W]_{\mathrm{org}}}{dt} = \frac{1}{1+K_W r_V}\left(k_2[F]_{\mathrm{org}}[S]_{\mathrm{org}} + k_3[F]_{\mathrm{org}}[A]_{\mathrm{org}} - k_5[F]_{\mathrm{org}}[W]_{\mathrm{org}} - k_{13}[A]_{\mathrm{org}}[W]_{\mathrm{org}} - 2k_{16}[W]_{\mathrm{org}}{}^2 - k_{17}[W]_{\mathrm{org}}[H]_{\mathrm{org}}\right),$$

$$\frac{d[H]_{\mathrm{org}}}{dt} = \frac{1}{1+K_H r_V}\left(k_1[F]_{\mathrm{org}}^2 + k_3[F]_{\mathrm{org}}[A]_{\mathrm{org}} - k_{10}[S]_{\mathrm{org}}[H]_{\mathrm{org}} + k_{11}[A]_{\mathrm{org}}^2 - k_{17}[W]_{\mathrm{org}}[H]_{\mathrm{org}}\right),$$

where $[F], [S], [A], [W]$, and $[H]$ indicate [^{Fuel}**PEG**], [**7-tetradecene** (Source)], [^{Amp}**PEG**], [**1-octene** (Waste)], and [^{Hyd}**PEG**], respectively. $k_i (i = 1, \ldots, 18)$ are chemical reaction rates; $r_V = \frac{V_{aq}}{V_{org}} = \frac{0.55}{0.26} = 2.12$ is the volume ratio of the aqueous phase to the organic phase; partition coefficients are $K_F = \frac{[F]_{\mathrm{aq}}}{[F]_{\mathrm{org}}}, K_S = \frac{[S]_{\mathrm{aq}}}{[S]_{\mathrm{org}}}$, $K_A = \frac{[A]_{\mathrm{aq}}}{[A]_{\mathrm{org}}}, K_W = \frac{[W]_{\mathrm{aq}}}{[W]_{\mathrm{org}}}$, and $K_H = \frac{[H]_{\mathrm{aq}}}{[H]_{\mathrm{org}}}$. The subscripts 'org' and 'aq' indicate 'in organic phase' and 'in aqueous phase', respectively. The partition coefficients K_F = 170, K_A = 0.18, and K_H = 18000 were experimentally determined (Fig. S16). $k_i (i = 1, 3, 5, 10, 11, 13, 16, \text{and } 17) = k_2 = 0.0179$ [min^{-1}M^{-1}] evaluated from Fig. 2b, and $k_i (i = 4, 6, 7, 8, 9, 12, 14, 15, \text{and } 18) = 0$. $[A]_{\mathrm{org}}(t = 0) = [K_W]_{\mathrm{org}}(t = 0) = [K_H]_{\mathrm{org}}(t = 0) = 0$ [mM]. In the case of the experiments with the organic and aqueous phases, $[S]_{\mathrm{org}}(t = 0) = 3.92$ [M], $[F]_{\mathrm{org}}(t = 0) = 94$ [mM]$\times \frac{r_V}{1+K_F r_V}$. In the case of the experiments with only the organic phase, $[S]_{\mathrm{org}}(t = 0) = 3.92$ [M] $\times \frac{0.26}{0.55+0.26} = 1.26$ [M], $[F]_{\mathrm{org}}(t = 0) = 116$ [mM] $\times$

$$\frac{0.55}{0.55+0.26} = 78.8 \text{ [mM]}.$$

Table S1 Possible reactions and their chemical reaction equations[a]

	F	S	A	W	H
F	$\mathbf{F + F \xrightarrow{k_1} H}$	$\mathbf{F + S \xrightarrow{k_2} A + W}$	$\mathbf{F + A \xrightarrow{k_3} W + H}$ $F + A \xrightarrow{k_4} F + A$	$\mathbf{F + W \xrightarrow{k_5} A}$	$F + H \xrightarrow{k_6} F + H$
S		$S + S \xrightarrow{k_7} S + S$	$S + A \xrightarrow{k_8} S + A$	$S + W \xrightarrow{k_9} S + W$	$\mathbf{S + H \xrightarrow{k_{10}} A + A}$
A			$\mathbf{A + A \xrightarrow{k_{11}} S + H}$ $A + A \xrightarrow{k_{12}} A + A$	$\mathbf{A + W \xrightarrow{k_{13}} S + F}$ $A + W \xrightarrow{k_{14}} A + W$	$A + H \xrightarrow{k_{15}} A + H$
W				$\mathbf{W + W \xrightarrow{k_{16}} S}$	$\mathbf{W + H \xrightarrow{k_{17}} A + F}$
H					$H + H \xrightarrow{k_{18}} H + H$

[a]Bold black reactions are significant reactions to model the chemical reaction network and grey reactions are insignificant. F: **^{Fuel}PEG**. S: Source (**7-tetradecene**). A: **^{Amp}PEG**. W: Waste (**1-octene**). H: **^{Hyd}PEG**. $k_i (i = 1, \ldots, 18)$: chemical reaction rates.

4.5. Evaluation of partition coefficients for 7-tetradecene–water biphasic system

7-tetradecene (500 µL) and an aqueous solution (500 µL) of **^{Fuel}PEG**, **^{Amp}PEG**, or **^{Hyd}PEG** ([**^{Fuel}PEG**] = 5 mM, [**^{Amp}PEG**] = 0.089 mM, [**^{Hyd}PEG**] = 6.7 mM; concentration of each compound was adjusted to be below the CAC) were vortexed for 10 min and then centrifuged (10,000 rpm) for at least 20 min at 20 °C. After separation of each layer, the aqueous phases were diluted 50-fold and 100-fold with water for **^{Fuel}PEG** and **^{Hyd}PEG**, respectively. The absorption spectra were measured at 20 °C using a quartz cell with an optical path length of 1 mm. The partition coefficients were calculated from the absorbance ratio of the aqueous phase to the organic phase (Fig. S16).

4.6. Analyses of emulsifying properties of ^{Fuel}PEG and ^{Hyd}PEG

7-tetradecene (105 mg) and an aqueous solution (275 μL) of **^{Fuel}PEG** or **^{Hyd}PEG** (**[^{Fuel}PEG]** = **[^{Hyd}PEG]** = 50 mM**)** were mixed in a glass tube and stirred for 4 h at room temperature. Photographs of the glass tubes were obtained before and after stirring (Fig. 3a and 3b). To quantify the emulsification properties, the resulting mixtures were transferred to 1.5 mL microcentrifuge tubes and allowed to stand for 1 min. Then, 50 μL of the bottom aqueous layer was transferred to a 96-well black/clear bottom microplate and the optical density (O.D.) was measured at λ = 600 nm using the microplate reader (Fig. S17).

4.7. Sample preparations for transmission electron microscopy (TEM)

An aqueous solution (1.5 μL) of **^{Amp}PEG** (1 mM) was deposited onto a copper TEM grid with a collodion film (200 mesh, EM Japan Co., LTD.) and held in place for 30 s. For **^{Fuel}PEG**, an aqueous solution (1.5 μL) of **^{Fuel}PEG** (30 mM, diluted 30 times with water right before the deposition) was used. The sample solutions were removed by capillary action using filter papers. The samples were then negatively stained with 1.5 μL of EM Stainer (gadolinium acetate, diluted 4 times with water) for 30 s, and the staining solutions were removed by capillary action using filter papers. The grids were dried overnight before imaging. The TEM micrographs are shown in Fig. 3d (**^{Fuel}PEG**) and Fig. S18 (**^{Amp}PEG**).

4.8. Determination of critical aggregation concentration (CAC)

To determine the CACs of **^{Fuel}PEG**, **^{Amp}PEG**, and **^{Hyd}PEG**, surface tension measurements of aqueous solutions of **^{Fuel}PEG**, **^{Amp}PEG**, and **^{Hyd}PEG** were performed at different concentrations at 25 °C using a tensiometer according to the pendant drop method.[S3] CACs were then determined from the intersections of the fitted lines of the obtained surface tension vs. concentration plots (Fig. 3e and S19).

4.9. Preparation of emulsions for microscopic observation

7-tetradecene (66 μL), an aqueous solution (137.6 μL) of **^{Fuel}PEG ([^{Fuel}PEG]** = 94 mM**)**, and HG- II (2.0 mg) were mixed in a glass tube and stirred for 30 min at room temperature. The bottom aqueous layer was taken using a pipette and was placed on a microplate for microscopic observation (Fig. S20).

4.10. Preparation of DiIC$_{18}$(3)-labeled giant unilamellar vesicles (GUVs)

DiIC$_{18}$(3)-labeled giant unilamellar vesicles (GUVs) were prepared according to the method analogous to that reported previously.[S4] A chloroform solution of 1,2-dioleoyl-*sn*-glycero-3- phosphocholine (DOPC, 6.0 mM, 100 μL), an ethanol solution of 1,1'-dioctadecyl-3,3,3',3'-tetramethylindocarbocyanine perchlorate (DiIC$_{18}$[3], 600 μM, 1.0 μL), and a methanol solution of glucose[S5] (12 mM, 50 μL) were mixed in a microtube, and the resulting mixture was deposited on an indium tin oxide (ITO)-coated glass slide. The film on the glass slide was dried overnight under reduced pressure. Then, the developed lipid film was sandwiched by another ITO-coated glass slide with a 0.1 mm-thick silicone-based spacer, and the film was hydrated with deionized water (300 μL). An AC voltage with an amplitude of 1.4 V and a frequency of 10 Hz was applied to the electrodes. After 2 h of an application of AC field, a dispersion of DiIC$_{18}$(3)-labeled GUVs ([DOPC] = 2.0 mM, [DiIC$_{18}$(3)] = 2.0 μM, [glucose] = 2.0 mM) was obtained. A fluorescence micrograph of the prepared DiIC$_{18}$(3)-labeled GUVs is shown in Fig. S21.

4.11. Microscopic observation of $DiIC_{18}(3)$-labeled GUVs in the presence of the reaction mixture

Following the same reaction procedure as described in section 4.2., the olefin metathesis of **^{Fuel}PEG** and **7-tetradecene** was performed in deionized water. The reaction kinetics analyzed by UPLC are shown in Fig. S22. At the reaction time points of 1, 60, and 120 min, 10 μL of the bottom aqueous layer of the reaction mixture was taken and diluted with deionized water (240 μL). Each sample was then vortexed for 10 s, transferred to a microtube, and centrifuged (100,000 rpm) for 2 h at 4 °C. The bottom aqueous layer (10 μL) of the centrifuged sample was added to the dispersion of $DiIC_{18}(3)$-labeled GUVs (30 μL, [DOPC] = 600 μM, [$DiIC_{18}(3)$] = 600 nM, [glucose] = 2.0 mM), and fluorescence micrographs of the mixtures were obtained (Fig. 4a, λ_{ex} = 520–550 nm, λ_{obsd} > 580 nm).

4.12. Preparation of large unilamellar vesicles (LUVs) for 5-CF leakage assay

A chloroform solution (1.2 mL) of DOPC (10 mM) in a glass tube was evaporated to dryness under reduced pressure for at least 1 h. A developed thin lipid film was then hydrated at 37 °C for 1 h with a HEPES buffer containing 5-CF ([HEPES] = 20 mM, [NaCl] = 50 mM, [5-CF] = 50 mM, pH 7.5, 1.2 mL), and vortexed for 1 min. After 5 freeze-to-thaw cycles, the resulting dispersion was extruded through a polycarbonate membrane with a pore diameter of 100 nm for 21 times at room temperate. The resulting dispersion was dialyzed at 4 °C in a HEPES buffer ([HEPES] = 20 mM, [NaCl] = 50 mM, pH 7.5) using Spectra/Por® Dialysis Membrane (MWCO 3500) to obtain 5-CF encapsulated in DOPC LUVs in HEPES buffer ([DOPC] = 10 mM, intravesicular [5-CF] = 50 mM, [HEPES] = 20 mM, [NaCl] = 50 mM, pH 7.5).[S6] The formation of monodisperse DOPC LUVs was confirmed by dynamic light scattering (DLS) measurement (Fig. S24a).

4.13. 5-CF leakage assay by fluorescence spectroscopy

Following the same reaction procedure as described in section 4.2., the olefin metathesis of **^{Fuel}PEG** and **7-tetradecene** was performed in deionized water. The reaction kinetics analyzed by UPLC are shown in Fig. 4c and S23. At the reaction time points of 1, 30, 60, 90, 120, and 150 min, 10 μL of the bottom aqueous layer of the reaction mixture was taken and diluted with deionized water (500 μL). Then, 10 μL of the mixture was added to the dispersion of 5-CF encapsulated in DOPC LUVs in HEPES buffer (2.0 mL, [DOPC] = 100 μM, [HEPES] = 20 mM, [NaCl] = 50 mM, pH 7.5) in a quartz cell and the mixture was stirred for 5 min. The fluorescence spectra of the mixtures were then recorded at 20 ºC (λ_{ex} = 490 nm) (Fig. 4b and 4c).

4.14. Preparation of LUVs for dynamic light scattering (DLS) measurements

A chloroform solution (150 μL) of DOPC (10 mM) in a glass tube was evaporated to dryness under reduced pressure for at least 1 h. A developed thin lipid film was then hydrated at 37 °C for 1 h with a HEPES buffer ([HEPES] = 20 mM, [NaCl] = 50 mM, pH 7.5, 1.5 mL), and vortexed for 1 min. After 5 freeze-to-thaw cycles, the resulting dispersion was extruded through a polycarbonate membrane with a pore diameter of 100 nm for 21 times at room temperate to obtain a dispersion of DOPC LUVs in HEPES buffer ([DOPC] = 1.0 mM, [HEPES] = 20 mM, [NaCl] = 50 mM, pH 7.5).

4.15. DLS measurements of LUVs in the presence of the reaction mixture

Following the same reaction procedure as described in section 4.2., the olefin metathesis of **^{Fuel}PEG** and **7-tetradecene** was performed in deionized water. The reaction kinetics analyzed by UPLC are shown in Fig. S23. At the reaction time points of 1, 60, and 120 min, 10 μL of the bottom aqueous layer of the reaction mixture was taken and diluted with deionized water (500 μL). Then, 20 μL of the mixture was added to the dispersion of DOPC LUVs in HEPES buffer (200 μL, [DOPC] = 100 μM, [HEPES] = 20 mM, [NaCl] = 50 mM, pH 7.5) and stirred for 5min. The mixture was transferred to a disposable plastic microcuvette and intensity- and number-based particle-size distribution profiles were obtained at 20 °C (Fig. S25).

4.16. Preparation of the suspension of red blood cells (RBCs)

Fresh cow blood was purchased from Tokyo Shibaura Zouki, and suspension of red blood cells (RBCs) were prepared as follows. 4.0 mL of cow blood was centrifuged (1,000 G) for 10 min at 20 °C using a 15 mL centrifuge tube, and 2.4 mL of the supernatant was removed. Then, 6.4 mL of phosphate-buffered saline (PBS, pH 7.4) was added, gently shaken by hand, centrifuged again (1,000 G) for 10 min at 20 °C, and 6.4 mL of the supernatant was removed. This washing procedure was repeated two more times. Then, 2.4 mL of PBS was added to the resulting suspension and gently shaken by hand. Finally, 2.0 mL of the suspension was diluted with 58 mL of PBS to obtain the suspension of RBCs for the hemolysis assay.[S7]

4.17. Hemolysis assay

Following the same reaction procedure as described in section 4.2., the olefin metathesis of **^{Fuel}PEG** and **7-tetradecene** was performed in deionized water. The reaction kinetics analyzed by UPLC are shown in Fig. 4d and S23. At the reaction time points of 1, 30, 60, 90, 120, and 150 min, 10 μL of the bottom aqueous layer of the reaction mixture was taken and diluted with deionized water (500 μL). Then, 10 μL of the mixture was added to the suspension of RBCs (300 μL) and incubated at 37 °C for 30 min. The resulting mixture was transferred to a 1.5 mL microcentrifuge tube and centrifuged

(1,000 G) for 10 min at 20 °C. Then, 100 μL of the supernatant was transferred to 96-well black/clear bottom microplate and the optical density (O.D.) was measured at λ = 540 nm using the microplate reader (Fig. 4d).[S7] In addition, 20 μL of the supernatant was diluted with 1.8 mL PBS and its absorption spectrum was measured at 20 ºC using a quartz cell with an optical path length of 5 mm (Fig. S28).

5. Supplementary Data

5.1. Kinetic analyses using UPLC

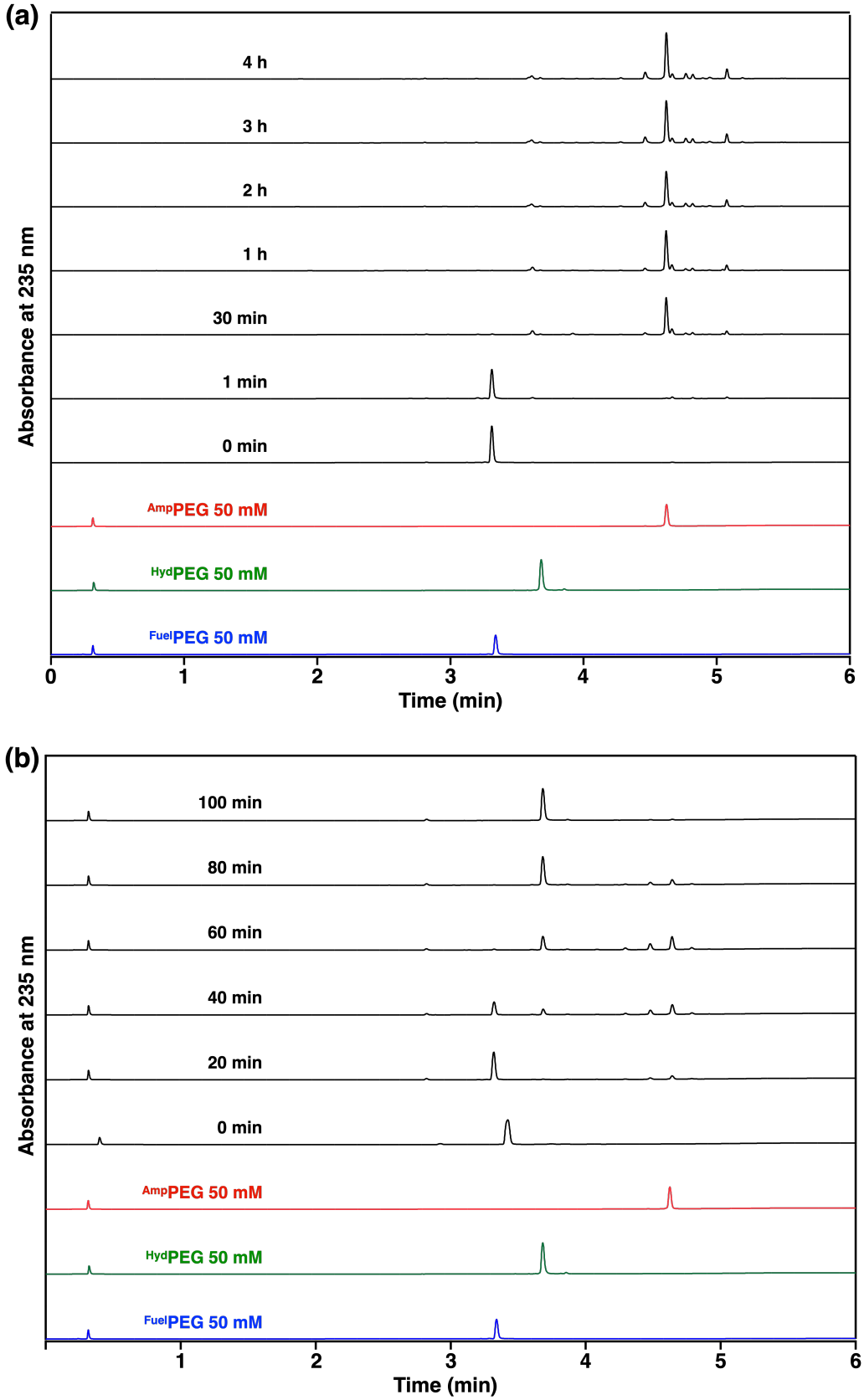

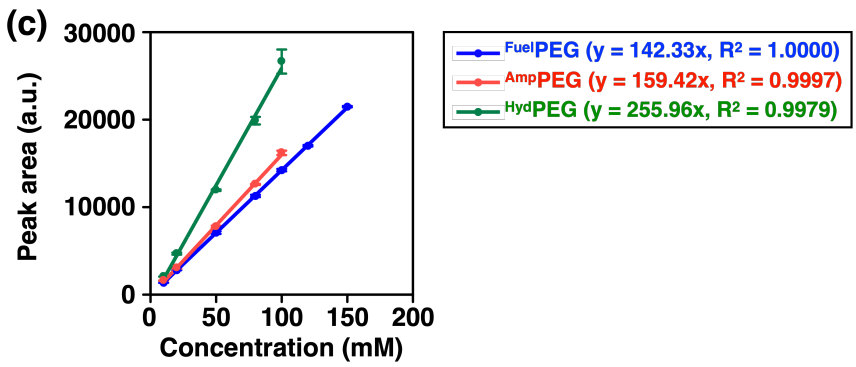

Fig. S14 (a and b) Representative UPLC trances obtained from the reaction mixture using (a) CH_2Cl_2 and (b) H_2O as solvent (detection wavelength: λ = 235 nm). UPLC trances obtained from authentic samples of **^{Fuel}PEG**, **^{Amp}PEG**, and **^{Hyd}PEG** are shown in the bottom of each figure. Note that minor peaks at 0.3 min are due to phloroglucinol used as an internal standard. (c) Plots of the concentration of **^{Fuel}PEG**, **^{Amp}PEG**, and **^{Hyd}PEG** prepared as standard samples as a function of the peak areas observed in UPLC analyses. Error bars represent the standard deviation (n = 3).

5.2. Concentration vs. time plots from qualitative kinetic simulation

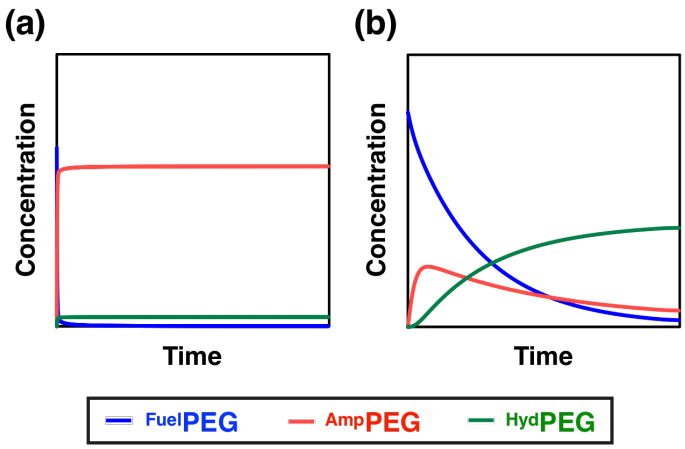

Fig. S15 (a) Concentration vs. time plot obtained from qualitative kinetic simulation under homogeneous conditions. (b) Concentration vs. time plot obtained from qualitative kinetic simulation under biphasic conditions.

5.3. Absorption spectral study for evaluation of partition coefficients

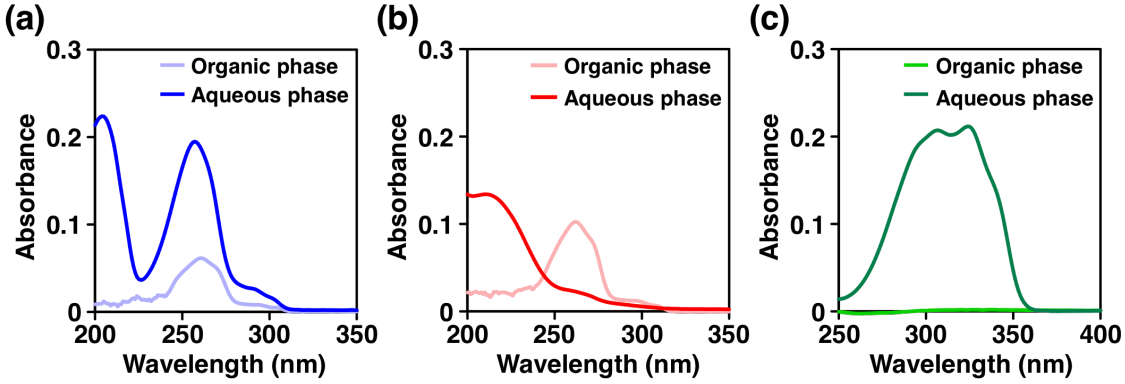

Fig. S16 (a-c) Representative absorption spectra of 7-tetradecene and an aqueous phase of (a) ^{Fuel}**PEG** (organic phase: pale blue, aqueous phase: blue, diluted 50 times with water), (b) ^{Amp}**PEG** (organic phase: pale red, aqueous phase: red), and (c) ^{Hyd}**PEG** (organic phase: pale green, aqueous phase: green, diluted 100 times with water) at 20 °C. The partition coefficients were determined from the average (n = 3) of the absorbance at 257, 262, and 324 nm, for ^{Fuel}**PEG** (K_F = 170 ± 17), ^{Amp}**PEG** (K_A = 0.18 ± 0.043), and ^{Hyd}**PEG** (K_H = 18000 ± 9600), respectively.

5.4. O.D. measurements of the emulsions formed by 7-tetradecene and ^{Fuel}PEG or ^{Hyd}PEG

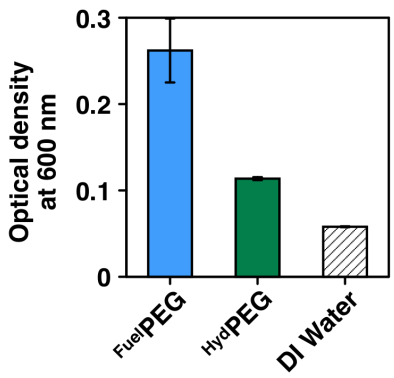

Fig. S17 O.D. at 600 nm of the emulsions formed by **7-tetradecene** and ^{Fuel}**PEG** (blue) or ^{Hyd}**PEG** (green). The O.D. of the mixture of **7-tetradecene** and deionized water is shown as a control (diagonal line pattern). Error bars represent the standard deviation (n = 3).

5.5. TEM micrograph of ^{Amp}PEG

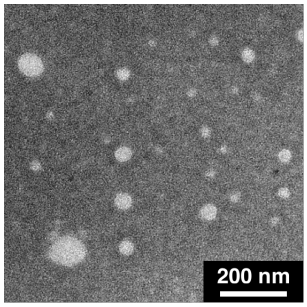

Fig. S18 TEM micrograph of an aqueous ^{Amp}**PEG** ([^{Amp}**PEG**] = 1 mM), negatively stained with gadolinium acetate. Scale bar: 200 nm.

5.6. Determination of CACs of ^{Amp}PEG and ^{Hyd}PEG by surface tension measurements

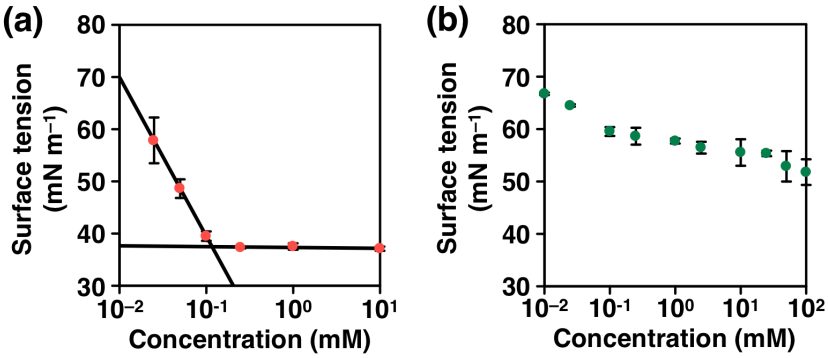

Fig. S19 Surface tension vs. concentration plots of aqueous (a) ^{Amp}**PEG** (red) and (b) ^{Hyd}**PEG** (green). The CAC of ^{Amp}**PEG** was determined from the intersection of the fitted lines ([^{Amp}**PEG**]$_{CAC}$ = 0.116 mM). Error bars represent the standard deviation (n = 10). CAC of ^{Hyd}**PEG** could not be determined due to its inability to self-assemble.

5.7. Optical micrograph of emulsions

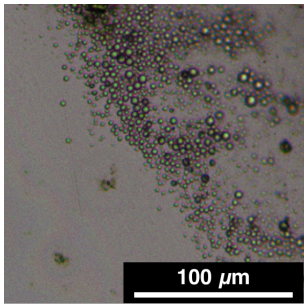

Fig. S20 An optical micrograph of emulsions formed by 7-tetradecene (66 μL), an aqueous solution of ^{Fuel}**PEG** (94 mM, 137.6 μL), and HG-II (2.0 mg) at 25 °C.

5.8. Fluorescence micrograph of $DiIC_{18}(3)$-labelled GUVs

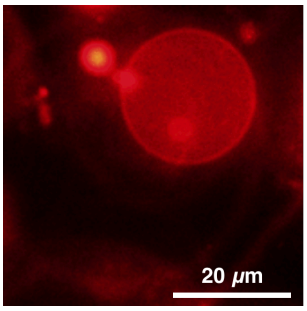

Fig. S21 A fluorescence micrograph of $DiIC_{18}(3)$-labeled GUVs ([DOPC] = 600 μM, [$DiIC_{18}(3)$] = 600 nM) in aqueous glucose (2.0 mM) at 25 °C (λ_{ex} = 520–550 nm, λ_{obsd} > 580 nm). The sample was diluted with aqueous glucose (2.0 mM) right before the observation.

5.9. Kinetic analysis of the reaction mixture used for microscopic observations of $DiIC_{18}(3)$-labelled GUVs

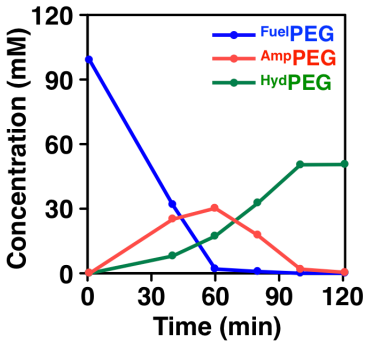

Fig. S22 Concentration vs. time plot of the biphasic reaction mixture used for microscopic observation of $DiIC_{18}(3)$-labelled GUVs. Reaction conditions are the same as the procedure as described in section 4.2. Reaction mixtures at 1, 60, and 120 min were used for microscopic observations.

5.10. Kinetic analysis of the reaction mixture used for 5-CF leakage assay, DLS analysis of LUVs, and hemolysis assay

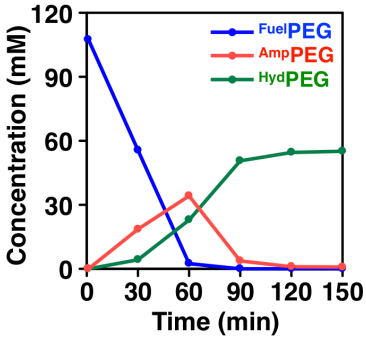

Fig. S23 Concentration vs. time plot of the biphasic reaction mixture used for DLS analysis of LUVs, 5-CF leakage assay, and hemolysis assay. HG-II was added after stirring the reaction mixture for 2 h at 50 °C. Other reaction conditions are the same as the procedure as described in section 4.2.

5.11. DLS analysis of LUVs and their release profiles of 5-CF in the presence of authentic samples of ^{Fuel}PEG, ^{Amp}PEG, and ^{Hyd}PEG

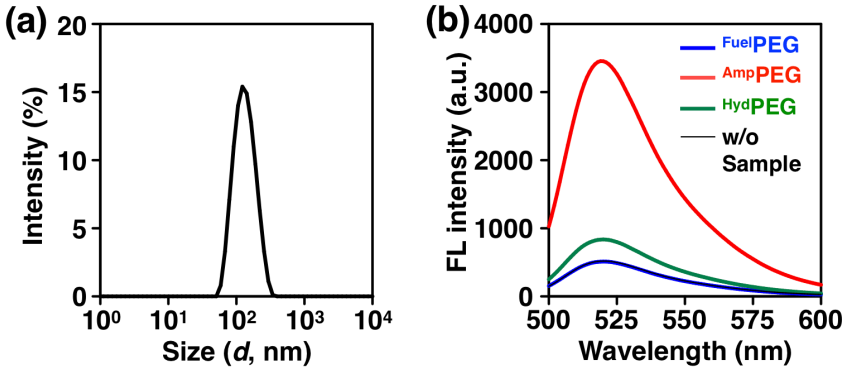

Fig. S24 (a) An intensity-based particle size distribution profile of DOPC LUVs encapsulating 5-CF in HEPES buffer ([DOPC] = 100 μM, intravesicular [5-CF] = 50 mM, [HEPES] = 20 mM, [NaCl] = 50 mM, pH 7.5) at 20 °C, analyzed by DLS. Mean hydrodynamic diameter of the particle: 127.2 nm. (b) Representative fluorescence spectra of 5-CF encapsulated in DOPC LUVs ([DOPC] = 100 μM, intravesicular [5-CF] = 50 mM, [HEPES] = 20 mM, [NaCl] = 50 mM, pH 7.5) after addition of aqueous ^{Fuel}**PEG** (10 mM, 10 μL, blue), ^{Amp}**PEG** (10 mM, 10 μL, red), ^{Hyd}**PEG** (10 mM, 10 μL, green), and that in the absence of additive (black) (λ_{ex} = 490 nm, λ_{em} = 520 nm) at 20 °C.

5.12. DLS analysis of LUVs in the presence of the reaction mixtures

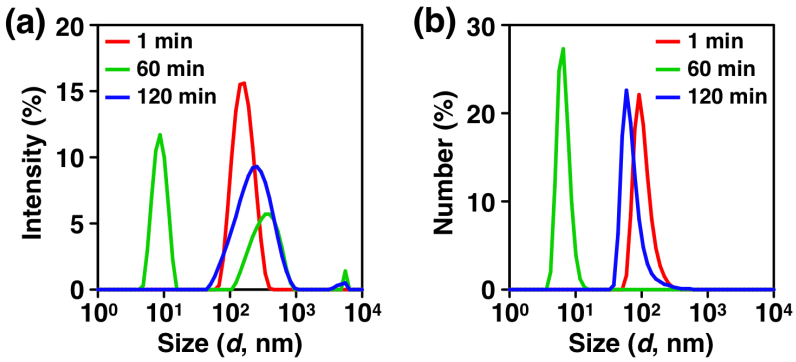

Fig. S25 (a) Intensity- and (b) number-based particle-size distribution profiles of DOPC LUVs in the presence of the reaction mixtures at different reaction times (1 min: red, 60 min: light green, 120 min: blue) at 20 °C, analyzed by DLS.

5.13. DLS analysis of ^{Amp}PEG

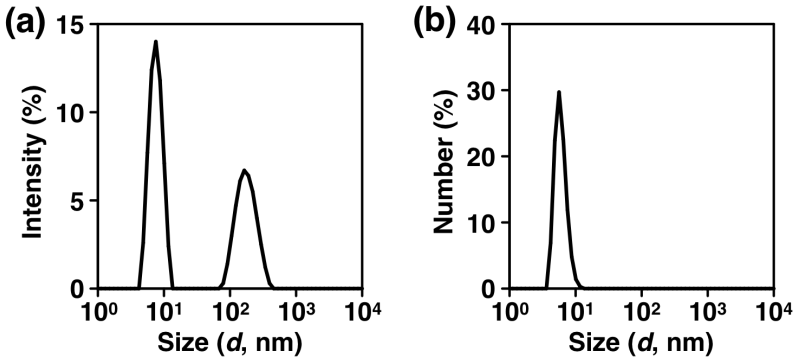

Fig. S26 (a) Intensity- and (b) number-based particle-size distribution profiles of aqueous ^{Amp}**PEG** ([^{Amp}**PEG**] = 7.6 mM) at 20 °C, analyzed by DLS. The mean hydrodynamic diameter of the particle was calculated to be 7.6 and 7.2 nm for intensity- and number-based analyses, respectively.

5.14. O.D. measurements of the suspensions of RBCs in PBS buffer in the presence of ^{Fuel}PEG, ^{Amp}PEG, and ^{Hyd}PEG

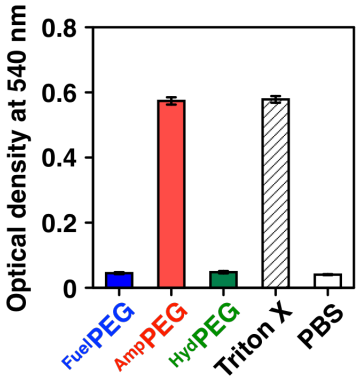

Fig. S27 Optical densities at 540 nm in the presence of ^{Fuel}**PEG** (10 mM, 10 μL, blue), ^{Amp}**PEG** (10 mM, 10 μL, red), ^{Hyd}**PEG** (10 mM, 10 μL, green), and Triton X-114 (50 mM, 10 μL, diagonal line pattern), and that in the absence of additive (white). Error bars represent the standard deviation (n = 5).

5.15. Absorption spectral study for denaturation of hemoglobin by authentic sample of ^{Amp}PEG and reaction mixtures

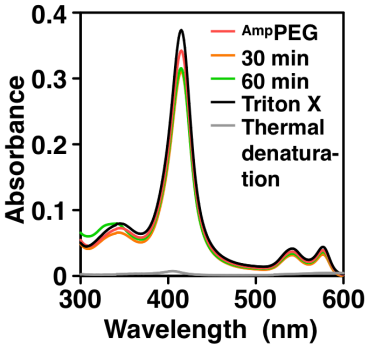

Fig. S28 Absorption spectra of supernatants after hemolysis by adding ^{Amp}**PEG** (red), reaction mixtures (30 min (orange) and 60 min (green)), and Triton X-114 (black). For the thermally denatured sample, the supernatant was heated at 80 °C for 10 min in the presence of Triton X-114 (gray).

6. Reference

(S1) P.-Y. Chen, Y.-H. Wu, M.-H. Hsu, T.-P. Wang and E.-C. Wang, *Tetrahedron* 2013, **69**, 653–657.

(S2) A. M. Wawro, T. Muraoka and K. Kinbara, *Polym. Chem.* 2016, **7**, 2389–2394.

(S3) N. Sadhukhan, T. Muraoka, D. Abe, Y. Sasanuma, D. R. G. Subekti and K. Kinbara, *Chem. Lett*. 2014, **43**, 1055–1057.

(S4) K. Sato, W. Ji, Z. Álvarez, L. C. Palmer and S. I. Stupp, *ACS Biomater. Sci. Eng.* 2019, **5**, 2786–2792.

(S5) K. Tsumoto, H. Matsuo, M. Tomita and T. Yoshimura, *Colloids Surf. B* 2009, **68**, 98–105.

(S6) R. Sasaki, K. Sato, K. V. Tabata, H. Noji and K. Kinbara, *J. Am. Chem. Soc.* 2021, **143**, 1348–1355.

(S7) J.-B. Wang, Y.-M. Wang and C.-M. Zeng, *Biochem. Biophys. Res. Commun.* 2011, **415**, 675–679.